

# Murine Corneal Inflammation and Nerve Damage After Infection With HSV-1 Are Promoted by HVEM and Ameliorated by Immune-Modifying Nanoparticle Therapy

Rebecca G. Edwards,<sup>1</sup> Sarah J. Kopp,<sup>1</sup> Igal Ifergan,<sup>1,2</sup> Jr-Wen Shui,<sup>\*,3</sup> Mitchell Kronenberg,<sup>3</sup> Stephen D. Miller,<sup>1,2</sup> and Richard Longnecker<sup>1</sup>

<sup>1</sup>Department of Microbiology and Immunology, Northwestern University Feinberg School of Medicine, Chicago, Illinois, United States

<sup>2</sup>Interdepartmental Immunobiology Center, Northwestern University Feinberg School of Medicine, Chicago, Illinois, United States

<sup>3</sup>Division of Developmental Immunology, La Jolla Institute for Allergy and Immunology, La Jolla, California, United States

Correspondence: Richard Longnecker, Ward 6-255, 303 E Chicago Avenue, Chicago, IL 60611, USA; r-longnecker@northwestern.edu. Stephen D. Miller, Tarry 6-713, 300 E Superior Street, Chicago, IL 60611, USA; s-d-miller@northwestern.edu.

Current affiliation: \*Institute of Biomedical Sciences, Academia Sinica, Taipei, Taiwan.

Submitted: September 2, 2016  
Accepted: November 17, 2016

Citation: Edwards RG, Kopp SJ, Ifergan I, et al. Murine corneal inflammation and nerve damage after infection with HSV-1 are promoted by HVEM and ameliorated by immune-modifying nanoparticle therapy. *Invest Ophthalmol Vis Sci.* 2017;58:282–291. DOI: 10.1167/iops.16-20668

**PURPOSE.** To determine cellular and temporal expression patterns of herpes virus entry mediator (HVEM, *Tnfrsf14*) in the murine cornea during the course of herpes simplex virus 1 (HSV-1) infection, the impact of this expression on pathogenesis, and whether alterations in HVEM or downstream HVEM-mediated effects ameliorate corneal disease.

**METHODS.** Corneal HVEM levels were assessed in C57BL/6 mice after infection with HSV-1(17). Leukocytic infiltrates and corneal sensitivity loss were measured in the presence, global absence (HVEM knockout [KO] mice; *Tnfrsf14*<sup>-/-</sup>), or partial absence of HVEM (HVEM conditional KO). Effects of immune-modifying nanoparticles (IMPs) on viral replication, corneal sensitivity, and corneal infiltrates were measured.

**RESULTS.** Corneal HVEM<sup>+</sup> populations, particularly monocytes/macrophages during acute infection (3 days post infection [dpi]) and polymorphonuclear neutrophils (PMN) during the chronic inflammatory phase (14 dpi), increased after HSV-1 infection. Herpes virus entry mediator increased leukocytes in the cornea and corneal sensitivity loss. Ablation of HVEM from CD45<sup>+</sup> cells, or intravenous IMP therapy, reduced infiltrates in the chronic phase and maintained corneal sensitivity.

**CONCLUSIONS.** Herpes virus entry mediator was expressed on two key populations: corneal monocytes/macrophages and PMNs. Herpes virus entry mediator promoted the recruitment of myeloid cells to the cornea in the chronic phase. Herpes virus entry mediator-associated corneal sensitivity loss preceded leukocytic infiltration, suggesting it may play an active role in recruitment. We propose that HVEM on resident corneal macrophages increases nerve damage and immune cell invasion, and we showed that prevention of late-phase infiltration of PMN and CD4<sup>+</sup> T cells by IMP therapy improved clinical symptoms and mortality and reduced corneal sensitivity loss caused by HSV-1.

Keywords: herpes simplex keratitis, immunopathology, nanoparticle

Herpes simplex virus 1 (HSV-1) is a neurotropic human pathogen causing a wide range of disease states from mild orolabial lesions, the most common manifestation, to deadly encephalitis and meningitis.<sup>1</sup> Another potentially devastating outcome of HSV-1 infection is herpes stromal keratitis (HSK), a recurrent syndrome in which chronic inflammation initiated by the virus produces corneal scarring, opacification, neovascularization, and potentially loss of vision.<sup>2–4</sup> Although actively replicating HSV-1 is required for HSK,<sup>5–7</sup> a pathologic immune response driven primarily by neutrophils and CD4<sup>+</sup> T cells develops that is sustained in the absence of replicating virus.<sup>8,9</sup> Understanding the virus-host interactions that together produce this pathogen-provoked immunoinflammatory syndrome is critical for the development of new, targeted therapies.

Herpes virus entry mediator (HVEM), a tumor necrosis factor receptor superfamily member, is a cellular receptor that stands at the intersection of viral pathogenesis and host immune responses. Originally identified as one of several gD-

receptors required for HSV entry,<sup>10–12</sup> HVEM facilitates viral entry in cultured human corneal and conjunctival epithelial cells,<sup>13,14</sup> as well as in primary human monocytes<sup>15</sup> and dendritic cells.<sup>16</sup> While HVEM is required for ocular pathogenesis *in vivo*,<sup>17</sup> the immunomodulatory effects of this receptor are more potent than its entry functions: HVEM increases corneal inflammatory cytokine production and leukocytic infiltration independently of viral entry.<sup>18–20</sup> Herpes virus entry mediator knockout (KO) mice have lower viral loads in eye swabs and subsequent spread to the nervous system, and lessened or absent clinical symptoms, including neurologic disease, periocular lesions, and mortality.<sup>17,18,21</sup>

Herpes virus entry mediator expression in the anterior eye has previously been localized to the corneal epithelium and stroma.<sup>22</sup> Herpes virus entry mediator is also found on a wide range of leukocytes, including neutrophils, monocytes, dendritic cells, and CD4<sup>+</sup> and CD8<sup>+</sup> T cells, although the expression of HVEM on these cells once in the cornea has



not been assessed.<sup>23,24</sup> We recently have found that HVEM-dependent disease after HSV-1 infection at the corneal surface is mediated by a radiation-resistant cell type or types,<sup>18</sup> leading us to hypothesize that HVEM on corneal epithelial cells, stromal fibroblasts, or resident stromal macrophages, which incompletely turn over after irradiation,<sup>25</sup> may promote pathogenesis in our adoptive transfer model. We investigated the expression of HVEM on a variety of cell lineages before, during, and after acute HSV-1 infection and found that corneal monocytes/macrophages are the first population to express HVEM, followed by polymorphonuclear neutrophils (PMN), double-negative (DN) T cells, and CD4<sup>+</sup> T cells. Increases in corneal HVEM expression were associated with loss of corneal sensitivity and leukocytic infiltrates, while loss of HVEM<sup>+</sup> cells from the cornea, either by genetic ablation or by administration of immune-modifying particles (IMPs), improved disease. We propose that HVEM on corneal resident monocytes/macrophages is integral for the recruitment of PMNs and other inflammatory cells to the cornea as well as nerve damage and loss of corneal sensitivity. Treatment with IMPs prevents the mobilization of immune cells to the cornea without hindering viral clearance and could show promise as a new therapeutic for treatment of chronic inflammation in HSK.

## MATERIALS AND METHODS

### Ethics Statement

This study was performed according to recommendations in the Guide for the Care and Use of Laboratory Animals of the National Institutes of Health and adhered to the ARVO Statement for the Use of Animals in Ophthalmic and Vision Research. The Committee on the Ethics of Animal Experiments of the Northwestern University approved the protocol (protocol Nos. 2012-1738 and IS00001532). Ketamine/xylazine or isoflurane anesthesia was used during procedures to minimize suffering.

### Cells and Viruses

Plaque assays were performed and virus was propagated on African green monkey kidney cells (Vero) as previously described<sup>18</sup>; HSV-1 strain 17 was obtained from David Leib (Dartmouth Medical School, Hanover, NH, USA).

### Animal Procedures

The Animal Care and Use Committee at Northwestern University approved all procedures, in strict adherence to institutional and National Institutes of Health guidelines. Mice were maintained in a specific pathogen-free environment and were transferred to a containment facility after infection. Male 9- to 15-week-old C57BL/6, BALB/c, and *Tnfrsf14*<sup>-/-</sup> (HVEM KO) were used in the study. Conditional HVEM KO mice were generated by crossing B6.Tg(Vav1-icre)A2Kio mice (Jackson, Bar Harbor, ME, USA), which express Cre recombinase in all hematopoietic lineages, with transgenic HVEM<sup>fl/fl</sup> mice, which have loxP sites flanking exons 3 and 6 of the *Tnfrsf14* gene (J-WS and MK, manuscript in preparation). Corneas were inoculated with  $2 \times 10^6$  plaque forming units (PFU) of HSV-1 in 5  $\mu$ L Dulbecco's modified Eagle's medium (DMEM) after scarification with a 25G needle in a crosshatch pattern as previously described; mock-infected controls instead received a Vero cell lysate after scarification to control for any effects mediated by free DNA and other cellular debris that may be present in the viral preparation.<sup>17,18</sup>

### Eye Swabs and Viral Plaque Assay

Eye swabs were collected as previously described into 1 mL DMEM media (DMEM containing 5% (vol/vol) fetal bovine serum (FBS), 1% gentamicin, 1% ciprofloxacin, and 1% amphotericin B) and stored at  $-80^{\circ}\text{C}$ .<sup>18</sup> Samples were thawed and vigorously vortexed for 30 seconds, and titers were determined with a standard plaque assay on Vero cells.

### Immunohistochemistry

Whole eyes were collected 1 day post infection (dpi), rinsed with phosphate-buffered saline (PBS), floated in 10% formalin + neutral buffered PBS for 24 hours, transferred to 70% ethanol, and stored at  $4^{\circ}\text{C}$  until paraffin embedding. Serial 4- $\mu$ m-thick sections were mounted on glass slides. The Northwestern University Mouse Histology and Phenotyping Laboratory provided naïve murine spleen controls. The following antibodies and concentrations were used for immunohistochemical (IHC) staining: rabbit polyclonal antibody (Patricia Spear, Northwestern University) or mouse monoclonal antibody (clone HMHV-1B18; BioLegend, San Diego, CA, USA) anti-HVEM antibodies diluted 1:200. Antigen retrieval was performed manually with Biocare (Birmingham, UK) decloaker for 5 minutes at  $100^{\circ}\text{C}$  followed by citrate buffer (pH 6.0). Secondary antibodies labeled with horseradish peroxidase (HRP) were visualized after treatment with chromogen diaminobenzidine (Vector Labs, Burlingame, CA, USA). After washing, slides were stained with Gill's Hematoxylin and imaged on the EVOS XL Core Imaging System (Thermo Fisher Scientific, Carlsbad, CA, USA).

### Flow Cytometry

Corneal pairs and spleens from individual mice were collected in cold PBS. Corneas were digested in 0.7 mg/mL Liberase (Roche, Indianapolis, IN, USA) in RPMI media for 1 hour in a  $37^{\circ}\text{C}$ , 5%  $\text{CO}_2$  incubator. Using a 1-mL syringe plunger, corneas were homogenized on top of a 100- $\mu$ m mesh, washed with cold PBS, strained through a 40- $\mu$ m mesh, and collected into a small volume. Spleens were prepared similarly to the corneas, but with a red blood cell lysis step between straining steps. After obtaining live cell counts, all of each cornea sample and a portion of each spleen sample were incubated with a 1:1000 dilution of Live/Dead Fixable Aqua Dead Cell Stain Kit (Thermo Fisher Scientific) in PBS in the dark at RT for 30 minutes. Samples were washed with PBS and incubated with Fc block (0.5–1.0  $\mu$ g/sample anti-mouse CD16/CD32 [eBioscience, San Diego, CA, USA] in PBS + 1% fetal bovine serum + 0.1% sodium azide [FACS buffer]) for 5 minutes at  $4^{\circ}\text{C}$  in the dark. Conjugated antibodies (2  $\mu$ g/mL final per sample) added directly to Fc block were incubated for 1 hour at  $4^{\circ}\text{C}$  in the dark. The following antibodies (and isotype controls) were used: HVEM-APC (HMHV-1B18), Ly6G Brilliant Violet 421 (1A8), CD8a Brilliant Violet 421 (53-6.7), E-cadherin-PE (DECMA-1), CD31-PB (390), IgG2 $\alpha$ k isotype control-Brilliant Violet (421): BioLegend; CD45-FITC (30-F11), CD3-APC eFluor 780 (17A2), CD11b-PECy7 (M1/70), CD11c-PE (N418), Ly6C-PerCP-Cy5.5 (HK1.4), CD4-PE (GK1.5), CD3e-PECy7 (145-2C11), Armenian hamster IgG isotype control-APC (eBio299Arm), rat IgG2 $\beta$ k isotype control-PerCP eFluor 710 (eB149/10HS), rat IgG $\alpha$  isotype control-APC eFluor 780 (eBR2a), ICAM-1-FITC (YN1/1.7.4), rat IgG2 $\beta$ k isotype control-FITC (eB149/10H5): eBioscience; NK1.1-APC Cy7 (PK136): BD Biosciences (San Jose, CA, USA). Samples were washed and resuspended in 200  $\mu$ L FACS buffer. Samples were collected on a FACS Canto II (BD Biosciences); the entire corneal pair sample was run, while spleen sample collection

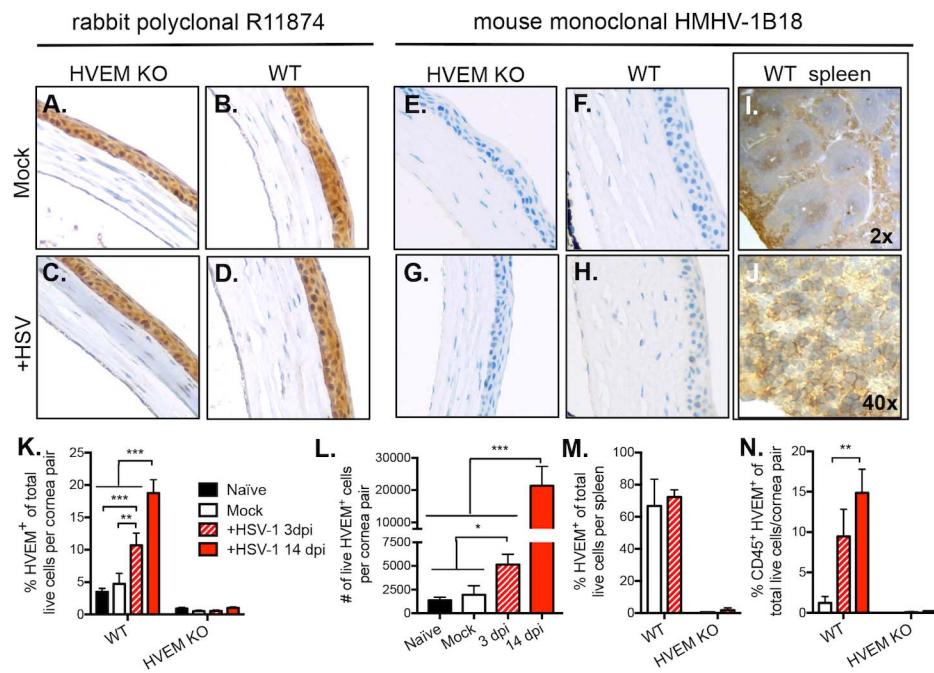


**FIGURE 1.** Herpes virus entry mediator expression increases in the murine cornea after HSV-1 infection. (A–J) Representative immunohistologic analysis of adult C57BL/6 (WT) or *Tnfrsf14*<sup>-/-</sup> (HVEM KO) eyes 1 day after scarification and mock-infection (Vero cell lysate control) (A, B, E, F) or infection (C, D, G, H) at the corneal surface with  $2.0 \times 10^6$  PFU/5  $\mu$ L per eye of HSV-1 strain 17 (original magnification  $\times 400$ ). Formalin-fixed paraffin-embedded eyes were serially sectioned and stained for HVEM with a rabbit polyclonal antibody, R11874 (A–D), or with a mouse monoclonal antibody, HMHV-1B18 (E–H). (I, J) Naïve murine spleens stained with HMHV-1B18. (K) Percentage and (L) absolute number of HVEM<sup>+</sup> cells per cornea pair as determined by flow cytometry ( $n = 7$ –12 cornea pairs from individual mice, three replicates). (M) Percentage HVEM positive per spleen 3 dpi ( $n = 3$ ). (N) Percentage of CD45<sup>+</sup> HVEM<sup>+</sup> of total cells per cornea pair 3 dpi ( $n = 7$ –9, two replicates). Values for (K–N) are means  $\pm$  SEM. Statistically significant differences are indicated as follows: \*\* $P < 0.01$ , \*\*\* $P < 0.001$ , \*\*\*\* $P < 0.0001$  (2-way ANOVA with Holm-Sidak’s adjustment for multiple comparisons).

was stopped at 100,000 live cells, and data analysis was performed with FlowJo 10.1 software (Ashland, OR, USA).

### Corneal Sensitivity

A Luneau Cochet-Bonnet esthesiometer (No. WO-7760; Western Ophthalmics, Lynnwood, WA, USA) was used to determine the blink threshold of the central cornea. Animals were scruffed, and the length of the monofilament was varied from 6.0 to 0.5 cm and touched perpendicularly to the surface of the central cornea until the first inflection point. A positive response was recorded when two blinks or more were obtained out of three attempts. Absence of a blink response at 0.5 cm was scored as a 0. The same examiner performed all measurements.

### Immune-Modifying Nanoparticle Treatment

Negatively charged IMPs derived from poly(lactic-co-glycolic acid) (PLGA) were produced by Phosphorex. Immune-modifying nanoparticles were diluted to a previously established maximally effective concentration of 4.7 mg/mL in filtered PBS (0.94 mg total/mouse/injection); 200  $\mu$ L IMPs or PBS vehicle control were delivered intravenously for 5 days (starting 3 dpi) via tail-vein injection.<sup>26</sup> A control cohort of animals was killed <24 hours after the final dose for analysis of spleens.

### Statistics

Geometric means of cell populations (percentages or absolute numbers) and corneal blink threshold each day were compared by using multiple unpaired *t*-tests or 1-way ANOVA with Holm-Sidak’s multiple comparisons post hoc test.

Associations between corneal blink threshold and viral load or CD45<sup>+</sup>, PMN, or macrophage cell number were assessed via linear regression. Kaplan-Meier mortality curves were compared by using the log-rank test. All statistics were calculated by using the GraphPad Prism 6.0f software (La Jolla, CA, USA).

## RESULTS

### Herpes Simplex Virus 1 Infection Expands HVEM<sup>+</sup> Populations in the Cornea

From bone marrow chimera experiments, we localized HVEM-mediated pathogenesis to a radiation-resistant cell type or types.<sup>18</sup> We reinvestigated the expression of HVEM in the cornea by immunohistology and flow cytometry, as a previous report indicates that HVEM is widely expressed in the naïve murine corneal epithelium *in vivo*, and that its expression increases in the epithelium and stroma as early as 1 day after infection in BALB/c mice.<sup>22</sup> The same rabbit polyclonal anti-HVEM antibody, R11874 (Patricia Spear, Northwestern University), produced nonspecific, background staining of the corneal epithelium of both wild-type (WT, C57BL/6) and HVEM KO (*Tnfrsf14*<sup>-/-</sup>) 9- to 12-week-old male mice 1 dpi with  $2.0 \times 10^6$  PFU/5  $\mu$ L/eye HSV-1 strain 17 or post mock-infection (Vero cell lysate) after scarification (Figs. 1A–D). In contrast, a commercially available mouse monoclonal antibody to HVEM, HMHV-1B18 (BioLegend), produced little positive staining in the cornea 1 dpi (Figs. 1E–H). As a positive control for the monoclonal antibody, we tested HMHV-1B18 in naïve murine spleens, which were floridly positive for HVEM after staining (Figs. 1I, 1J), consistent with previously described expression on B cells, T cells, myeloid cells, dendritic cells (DCs), and

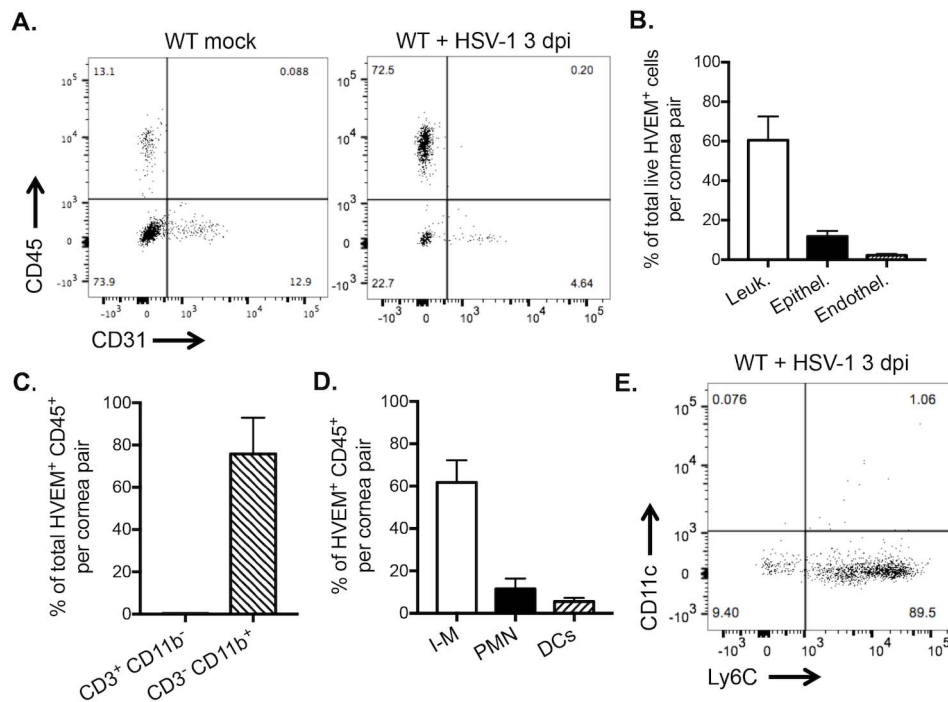


**FIGURE 2.** Acutely induced HVEM<sup>+</sup> cells in the infected murine cornea are mainly CD45<sup>+</sup>/CD3<sup>-</sup>/CD11b<sup>+</sup>/CD11c<sup>-</sup>/Ly6C<sup>+</sup>/Ly6G<sup>-</sup> monocytes. Three dpi, corneas from WT mice infected at the corneal surface with HSV-1(17) were analyzed for expression of HVEM, the pan-leukocyte marker CD45, the endothelial marker CD31, and the epithelial markers E-cadherin and ICAM via flow cytometry. (A) Representative dot plots of live HVEM<sup>+</sup> cells from mock and infected corneas for CD45 and CD31. (B) Percentage of total HVEM<sup>+</sup> cells from infected WT corneas that are CD45<sup>+</sup> leukocytes, CD45<sup>-</sup>/E-cadherin<sup>+</sup>/ICAM<sup>+</sup> epithelial cells, or CD45<sup>-</sup>/CD31<sup>+</sup> endothelial cells. Corneal isolates were also evaluated for leukocytic lineage markers, including CD3, CD11b, Ly6C, Ly6G, and CD11c. (C) Percentage of HVEM<sup>+</sup>/CD45<sup>+</sup> cells expressing the lymphoid marker CD3 or the myeloid marker CD11b 3 dpi. (D) Percentage of HVEM<sup>+</sup>/CD45<sup>+</sup>/CD3<sup>-</sup>/CD11b<sup>+</sup> myeloid cells categorized as inflammatory monocyte/macrophage lineage (I-Ms; CD11c<sup>-</sup>/Ly6C<sup>+</sup>/Ly6G<sup>-</sup>), PMNs (CD11c<sup>-</sup>/Ly6C<sup>+</sup>/Ly6G<sup>+</sup>), or dendritic cells (CD11c<sup>+</sup>/Ly6G<sup>-</sup>). (E) Representative dot plot of CD11c versus Ly6C expression of HVEM<sup>+</sup>/CD45<sup>+</sup>/CD3<sup>-</sup>/CD11b<sup>+</sup> myeloid cells from a WT cornea pair 3 dpi. Values for (B–E) are means ± SEM (*n* = 8 cornea pairs, two replicates).

other leukocytes.<sup>23</sup> These findings suggest HVEM expression in the corneas of C57BL/6 mice is limited immediately after scarification or infection.

We used flow cytometry to quantify HVEM expression in pairs of corneas from naïve, mock-infected, or infected adult WT or HVEM KO control mice 3 or 14 dpi (Fig. 1K; Supplementary Fig. S1). Herpes virus entry mediator KO samples, an isotype control antibody, and fluorescence minus one control were used to define the threshold for HVEM positivity. Wild-type corneas contained a significantly higher proportion (Fig. 1K) and greater absolute number (Fig. 1L) of HVEM<sup>+</sup> cells 3 and 14 dpi than naïve corneas or mock-infected corneas, and this increase was specific to the cornea, as no such expansion occurred in the spleen (Fig. 1M). Most of the expanded HVEM<sup>+</sup> population was attributable to an increase in HVEM<sup>+</sup>/CD45<sup>+</sup> cells both at 3 dpi and 14 dpi (compare Fig. 1K to 1N; Supplementary Fig. S1). These findings indicate that HVEM, rather than being highly expressed by the murine corneal epithelium, is limited to CD45<sup>+</sup> populations and is induced after infection with HSV-1 in a time-dependent manner.

### Most HVEM<sup>+</sup> Cells in the Acutely Infected Murine Cornea Derive From the Monocyte/Macrophage Lineage

To further characterize corneal HVEM expression, we analyzed HVEM<sup>+</sup> corneal isolates from adult WT mice 3 dpi for the pan-leukocyte marker CD45, the endothelial marker CD31, and the epithelial markers E-cadherin and ICAM-1 by flow cytometry.

Isotype controls were used to set thresholds for each. Mock-infected corneas contained few HVEM<sup>+</sup> cells, and few of those were CD45<sup>+</sup>, while the HVEM<sup>+</sup> cells from infected corneas 3 dpi were mostly CD45<sup>+</sup> leukocytes (Figs. 2A, 2B; Supplementary Fig. S1). Epithelial cells, defined in this study as CD45<sup>-</sup>/E-cadherin<sup>+</sup>/ICAM<sup>+</sup>, and endothelial cells (CD45<sup>-</sup>/CD31<sup>+</sup>) represented small portions of HVEM<sup>+</sup> cells in infected WT corneas; the remainder of HVEM<sup>+</sup> cells collected were not positive for any of these markers (Fig. 2B). The HVEM<sup>+</sup> leukocytes in infected corneal tissue 3 dpi were overwhelmingly CD3<sup>-</sup>/CD11b<sup>+</sup> myeloid cells (Fig. 2C; see Supplementary Fig. S3 for gating strategy), specifically Ly6G<sup>-</sup>/CD11c<sup>-</sup>/Ly6C<sup>+</sup> inflammatory monocytes/macrophages (Figs. 2D, 2E). Few were found to be Ly6G<sup>+</sup>/Ly6C<sup>+</sup>/CD11c<sup>-</sup> neutrophils (PMN) or Ly6G<sup>-</sup>/CD11c<sup>-</sup> myeloid dendritic cells (mDCs).

### Herpes Virus Entry Mediator Promotes Loss of Corneal Sensitivity and Corneal Leukocytic Infiltration

To determine whether the increase in HVEM<sup>+</sup> cells over the course of HSV-1 infection impacts corneal physiology and function, we determined the corneal touch threshold in WT and HVEM KO mice corneally infected with HSV-1(17) with a Luneau Cochet-Bonnet esthesiometer as previously described.<sup>27</sup> Briefly, the length of the filament was varied from 6 to 0.5 cm in increments of 0.5 cm and touched perpendicularly to the central cornea until the first inflection point. The blink threshold was counted as the length at which the animal blinked two times or more out of three; if no

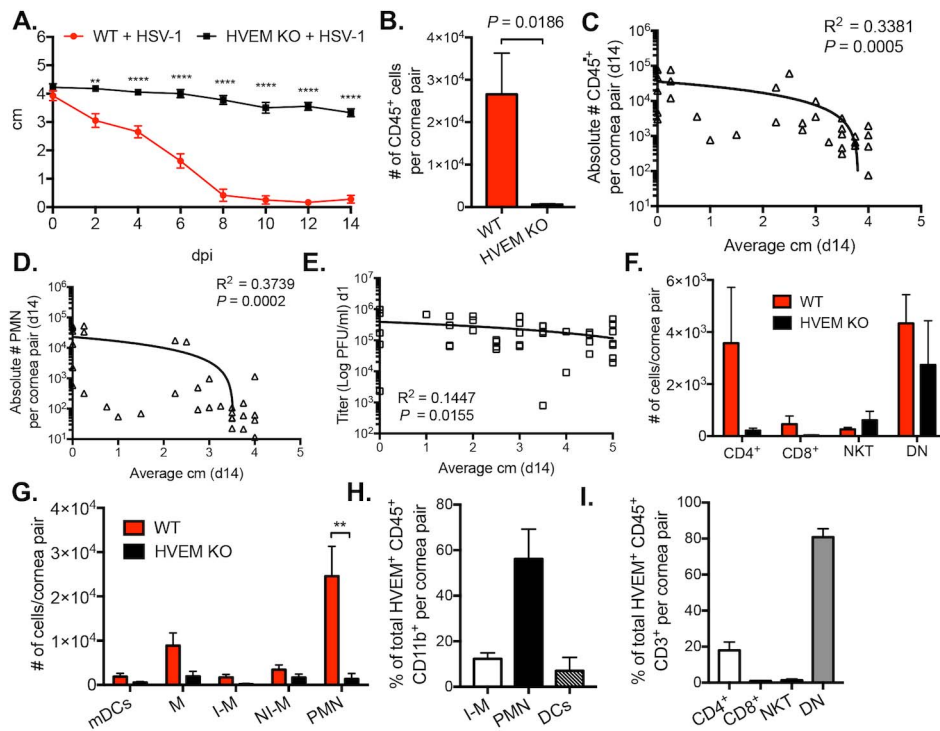


**FIGURE 3.** Herpes virus entry mediator-dependent loss of corneal sensitivity is associated with leukocytic infiltration of the cornea. (A) Corneal touch threshold was determined with a Luneau Cochet-Bonnet esthesiometer every other day beginning before infection (day 0) in WT or HVEM KO mice inoculated at the corneal surface with HSV-1(17). Lack of a blink reflex at 0.5 cm was recorded as 0 cm ( $n = 10$  mice per group, 20 individual corneas measured, two replicates). (B) Flow cytometry analysis of CD45<sup>+</sup> infiltrates in WT or HVEM KO corneas 14 dpi ( $n = 7-8$ , two replicates, 2-tailed  $t$ -test). (C) Relationship between corneal touch threshold on day 14 and the absolute number of corneal CD45<sup>+</sup> cells, (D) PMN, or (E) day 1 viral loads in the cornea ( $n = 32$ ,  $\geq 3$  individual experiments, linear regression for goodness of fit). (F) Absolute number of CD4<sup>+</sup> T cells (CD45<sup>+</sup>/CD3<sup>+</sup>/CD4<sup>+</sup>/CD8<sup>-</sup>), CD8<sup>+</sup> T cells (CD45<sup>+</sup>/CD3<sup>+</sup>/CD8<sup>+</sup>/CD4<sup>-</sup>), NKT cells (CD45<sup>+</sup>/CD3<sup>+</sup>/NK1.1<sup>+</sup>), or DN T cells (CD45<sup>+</sup>/CD3<sup>+</sup>/CD8<sup>-</sup>/CD4<sup>-</sup>/NK1.1<sup>-</sup>) or (G) the absolute number of mDCs (CD45<sup>+</sup>/CD3<sup>-</sup>/CD11b<sup>+</sup>/Ly6G<sup>-</sup>/CD11c<sup>+</sup>), monocytes/macrophages (Ms; CD45<sup>+</sup>/CD3<sup>-</sup>/CD11b<sup>+</sup>/Ly6G<sup>-</sup>/CD11c<sup>-</sup>), which were then further categorized as I-Ms (CD45<sup>+</sup>/CD3<sup>-</sup>/CD11b<sup>+</sup>/Ly6G<sup>-</sup>/CD11c<sup>-</sup>/Ly6C<sup>+</sup>) or noninflammatory monocytes/macrophages (NI-Ms; CD45<sup>+</sup>/CD3<sup>-</sup>/CD11b<sup>+</sup>/Ly6G<sup>-</sup>/CD11c<sup>-</sup>/Ly6C<sup>low</sup>), and finally PMNs (CD45<sup>+</sup>/CD3<sup>-</sup>/CD11b<sup>+</sup>/Ly6C<sup>+</sup>/Ly6G<sup>+</sup>) in WT versus HVEM KO corneas 14 dpi ( $n = 11$ ,  $\geq 3$  individual experiments). (H, I) Percentage of HVEM<sup>+</sup> corneal cells of the indicated cell lineage 14 dpi ( $n = 8$ , two replicates). Values in (A, B, D-F) are means  $\pm$  SEM, analyzed with 2-tailed  $t$ -test with Holm-Sidak's correction for multiple comparisons. \* $P < 0.05$ , \*\* $P < 0.01$ , \*\*\* $P < 0.001$ , \*\*\*\* $P < 0.0001$ .

response occurred at 0.5 cm, the eye was scored as 0. After infection, WT mice rapidly and dramatically lost sensitivity in the central cornea, compared to HVEM KO mice, in which corneal reflexes were largely maintained (Fig. 3A). Along with experiencing a loss of sensitivity, WT corneas also became more heavily infiltrated by CD45<sup>+</sup> leukocytes, as determined by flow cytometry on day 14 (Fig. 3B).

To determine if a correlation between these two factors existed, we performed a linear regression on the average blink threshold length at the end of the experiment, day 14, compared to the number of CD45<sup>+</sup> cells in the cornea on that same day (Fig. 3C), and found a significant negative association between these factors ( $R^2 = 0.338$ ,  $P = 0.0005$ ). Characterized by cell type, similar negative correlations also existed between number of PMNs (Fig. 3D) and number of monocytes/macrophages (data not shown) and the blink threshold length ( $R^2 = 0.374$ ,  $P = 0.0002$  and  $R^2 = 0.2992$ ,  $P = 0.0012$ , respectively). We collected eye swabs from infected mice 1, 3, and 5 dpi to determine viral loads in the tear film, and found lower day-1 titers from HVEM KO eye swabs than from WT (data not shown), similar to what we have previously reported.<sup>17</sup> Comparison of day 1 (but not day 3 or day 5) eye swab titers to the blink threshold (day 14) for each eye individually revealed a significant but small negative correlation (Fig. 3E;  $R^2 = 0.145$ ,  $P = 0.0155$ ).

We next investigated the specific identities of the CD45<sup>+</sup> populations in WT and HVEM KO corneas 14 dpi (see Fig. 2C; see Supplementary Figs. S2, S3 for gating strategy). Herpes simplex virus 1-infected WT corneas tended to contain higher populations of CD4<sup>+</sup> and CD8<sup>+</sup> T cells on day 14 than HVEM KO corneas, although these differences did not reach statistical significance (Fig. 3F). Levels of mDCs (CD45<sup>+</sup>/CD3<sup>-</sup>/CD11b<sup>+</sup>/Ly6G<sup>-</sup>/CD11c<sup>+</sup>), monocytes/macrophages (CD45<sup>+</sup>/CD3<sup>-</sup>/CD11b<sup>+</sup>/Ly6G<sup>-</sup>/CD11c<sup>-</sup>), and specifically, inflammatory monocytes/macrophages (Ly6C<sup>+</sup> monocytes/macrophages) in WT corneas were higher than in HVEM KO corneas to the 0.05 significance level, but after correction for multiple comparisons, only the level of PMNs remained statistically significantly higher in WT corneas than in HVEM KO corneas (Fig. 3G). Wild-type corneas tended to contain more CD4<sup>+</sup> and DN T cells, mDCs, and monocyte/macrophages than HVEM KO corneas during acute infection (5 dpi), although these differences were not statistically significant (data not shown). Polymorphonuclear neutrophils were notably absent from the corneas of both genotypes at this time point, consistent with previously published reports that neutrophils invade the cornea in two temporally distinct waves.<sup>28-30</sup>

At 14 dpi, most HVEM<sup>+</sup>/CD45<sup>+</sup> cells in WT corneas remained CD3<sup>-</sup>/CD11b<sup>+</sup> myeloid cells, although approximately 20% of HVEM<sup>+</sup>/CD45<sup>+</sup> cells were CD3<sup>+</sup> (data not shown). Most HVEM<sup>+</sup>/CD3<sup>-</sup>/CD11b<sup>+</sup> cells were PMNs, signaling a switch

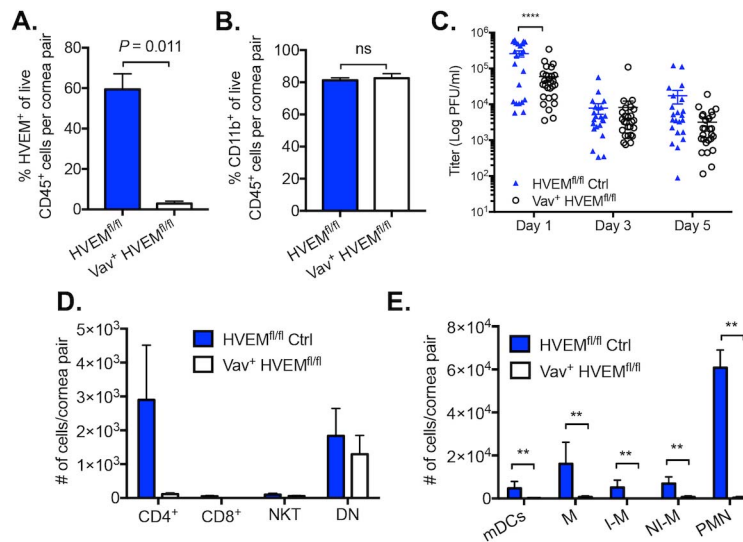


**FIGURE 4.** Loss of HVEM from CD45<sup>+</sup> lineages reduces myeloid infiltrates during the chronic inflammatory phase. Mice lacking HVEM specifically on CD45<sup>+</sup> cells were generated by crossing HVEM<sup>fl/fl</sup> mice with B6.Tg(Vav1-cre)A2Kio mice, which express Cre recombinase throughout the hematopoietic compartment. Adult mice were infected with HSV-1(17) after corneal scarification. **(A)** Confirmation of loss of HVEM expression on CD45<sup>+</sup> hematopoietic cells in the cornea 3 dpi in the conditional KO, the Cre-expressing homozygous floxed animals (Vav<sup>+</sup> HVEM<sup>fl/fl</sup>), compared to homozygous HVEM<sup>fl/fl</sup> controls. **(B)** Percentage of CD11b<sup>+</sup> myeloid cells of total CD45<sup>+</sup> cells 3 dpi in Vav<sup>+</sup> HVEM<sup>fl/fl</sup> or control HVEM<sup>fl/fl</sup> corneas. Values are means ± SEM, *n* = 2–3, 2-tailed *t*-test. **(C)** Titers in eye swabs collected 1, 3, and 5 dpi in Vav<sup>+</sup> HVEM<sup>fl/fl</sup> or control HVEM<sup>fl/fl</sup> corneas (*n* = 11–13 mice, three replicates). **(D)** Absolute number of CD4<sup>+</sup> T cells, CD8<sup>+</sup> T cells, NKT cells, or DN T cells, or **(E)** absolute number of mDCs, Ms, I-Ms, NI-Ms, or PMNs found in the corneas of conditional KO or control mice 14 dpi (*n* = 5–10, three replicates). All values are means ± SEM, (C–E) evaluated with 2-tailed *t*-tests with Holm-Sidak’s correction for multiple comparisons. \**P* < 0.05, \*\**P* < 0.01, \*\*\**P* < 0.001, \*\*\*\**P* < 0.0001.

from the acute phase infection, when corneal monocytes/macrophages represented the greatest HVEM<sup>+</sup> population (comparing Fig. 2D to Fig. 3H). Of HVEM<sup>+</sup>/CD3<sup>+</sup>/CD11b<sup>-</sup> cells, most were CD8<sup>-</sup>/CD4<sup>-</sup> (as well as NK1.1<sup>-</sup>) cells, here called DN T cells, although this population could potentially represent γδ T cells. A small population of HVEM<sup>+</sup>/CD4<sup>+</sup> also occurred in the cornea 14 dpi (Fig. 3D). These data indicate that HVEM promotes an increase in viral replication, as previously reported, as well as increased corneal infiltration, both of which correlated with a loss of central corneal sensitivity.

### Ablation of HVEM From CD45<sup>+</sup> Lineages Reduces Myeloid Infiltrates Late in Infection

We specifically ablated HVEM from CD45<sup>+</sup> cells by using a Cre/lox system. HVEM<sup>fl/fl</sup> mice on the C57BL/6 background contain loxP sites flanking exons 3 and 6 of the HVEM gene. These animals were bred to B6.Tg(Vav1-cre)A2Kio mice (Jackson), which express Cre recombinase under control of the Vav promoter, resulting in expression in 98% to 100% of hematopoietic cells with no littermate mosaicism.<sup>31</sup> Genotyping was performed by PCR analysis of floxed HVEM and Vav-Cre genes. In addition, we confirmed that homozygous floxed animals expressing Vav-Cre (Vav<sup>+</sup> HVEM<sup>fl/fl</sup>) had successful ablation of HVEM from CD45<sup>+</sup> cells in comparison to homozygous HVEM<sup>fl/fl</sup> controls by analysis of peripheral blood (data not shown) and infected corneas via flow cytometry for HVEM expression (Fig. 4A). Although CD11b<sup>+</sup> myeloid cells had lost HVEM expression, this did not impact the presence of CD11b<sup>+</sup> populations in the cornea 3 dpi (Fig. 4B). Consistent with HVEM KOs, Vav<sup>+</sup> HVEM<sup>fl/fl</sup> corneas had significantly lower titers than controls early after infection (Fig. 4C). We also assessed late-phase populations of corneal leukocytes to determine if HVEM-dependent infiltration required HVEM expression on CD45<sup>+</sup> cell types. Infiltration of CD4<sup>+</sup> and CD8<sup>+</sup> T cells was diminished in Vav<sup>+</sup> HVEM<sup>fl/fl</sup> mice compared to controls, although this did not reach statistical significance

(Fig. 4D). However, myeloid cell infiltration into the cornea 14 dpi was markedly blunted when HVEM was ablated from CD45<sup>+</sup> cells (Fig. 4E). Corneal sensitivity in Vav<sup>+</sup> HVEM<sup>fl/fl</sup> mice was also maintained, similar to that of HVEM KOs (data not shown). These findings suggest that the establishment of CD11b<sup>+</sup> myeloid cells in the cornea in the acute phase is HVEM independent, but that the recruitment or maintenance of myeloid lineages in the chronic phase of infection cannot occur effectively without HVEM.

### Negatively Charged IMP Treatment Ameliorates Disease After Ocular HSV-1(17) Infection

Negatively charged, 500-nm-diameter IMPs derived from PLGA limit tissue infiltration of inflammatory monocytes and other circulating phagocytic cells by rerouting them to the spleen for degradation.<sup>26</sup> Immune-modifying nanoparticle therapy is effective in a wide range of inflammatory diseases, including West Nile infection, experimental autoimmune encephalitis, cardiac and kidney reperfusion injury, and others.<sup>26</sup> Herpes virus entry mediator, which we found localized mostly on corneal inflammatory monocytes/macrophages during acute infection, and on PMNs during the chronic phase, promotes infiltration and is associated with sensory loss at the corneal surface. We hypothesized that IMP treatment could prevent the migration of circulating immune cells into the cornea, even in the presence of HVEM, and thus ameliorate corneal disease.

We performed a pilot study in adult male BALB/c mice, which are highly susceptible to neurologic morbidity after corneal HSV-1 infection, to determine if a previously established dose of 0.94 mg IMPs/mouse via tail-vein injection delivered daily for 5 days could improve survival when compared to mice receiving the vehicle, PBS. To target the later, pathologic influx of immune cells without hindering viral clearance, we began treatment 3 dpi, before the onset of clinical symptoms such as ruffled fur, periorbital swelling, and lesion development, which occur around day 5,<sup>17</sup> but after an

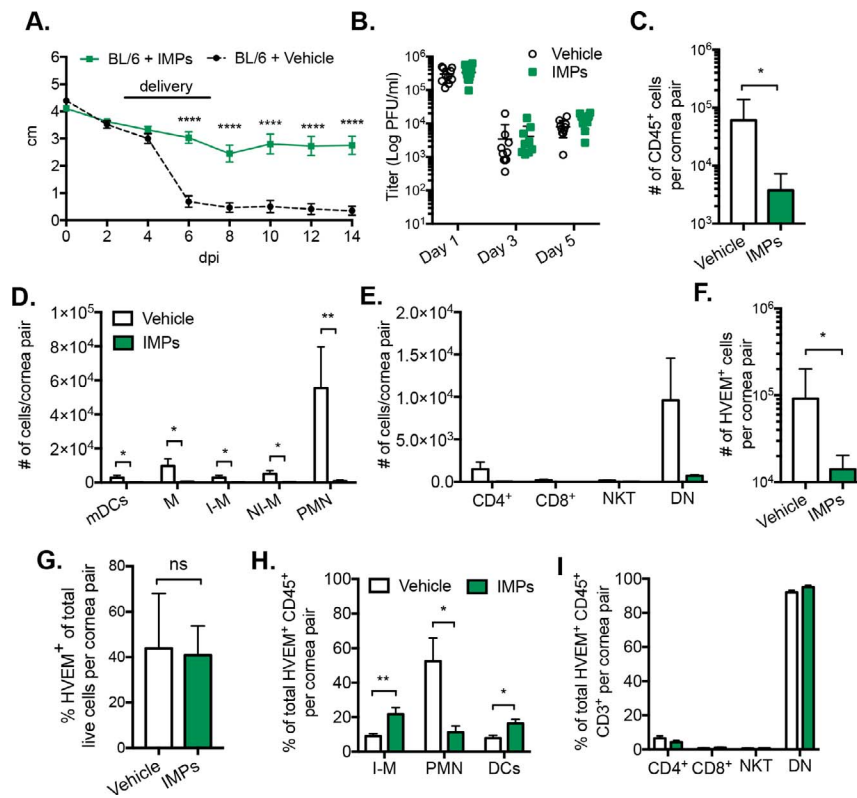


**FIGURE 5.** Treatment with negatively charged IMPs ameliorates disease and reduces corneal infiltrates after ocular HSV-1(17) infection. C57BL/6 mice were inoculated with  $2.0 \times 10^6$  PFU/5  $\mu$ L per eye of HSV-1(17) after corneal scarification and treated with 200  $\mu$ L vehicle control (PBS) or negatively charged IMPs for 5 days starting 3 dpi. **(A)** Corneal touch threshold of C57BL/6 mice with or without IMP treatment (determined with a Lunau Cochet-Bonnet esthesiometer,  $n = 10$  individual mice, 20 corneas tested, two replicates). **(B)** Viral loads in the tear film of C57BL/6 mice with or without IMP treatment ( $n = 10$ ). **(C-F)** Absolute numbers of the indicated cell population present in IMP- or sham-treated corneas 14 dpi as determined by flow cytometry. **(G)** Percentage of total cells that are HVEM<sup>+</sup> in treated or sham-treated mice. **(H, I)** Percentage of HVEM<sup>+</sup> cells belonging to each population ( $n = 10$  for [D-I], two replicates, values are means  $\pm$  SEM, 2-tailed *t*-test with Holm-Sidak's correction for multiple comparisons). \* $P < 0.05$ , \*\* $P < 0.01$ , \*\*\* $P < 0.001$ , \*\*\*\* $P < 0.0001$ .

innate response had been mounted.<sup>2,32-34</sup> Treated mice survived at significantly higher rates (40% vs. 0%) than mice that received the vehicle (data not shown). We next tested the therapeutic potential of IMPs in C57BL/6 mice to prevent loss of corneal sensitivity, reduce corneal infiltration, and improve symptoms after HSV-1 infection. Immune-modifying nanoparticle-treated mice maintained corneal blink thresholds similar to preinfection levels, while corneal sensitivity in vehicle-treated animals significantly declined by 6 dpi (Fig. 5A). Viral titers in eye swabs collected 1, 3, and 5 dpi did not differ between the treatment groups (Fig. 5B).

Flow cytometry of corneas collected on day 14 revealed that IMP treatment significantly reduced CD45<sup>+</sup> populations (Fig. 5C), particularly in all myeloid populations we investigated (Fig. 5D), and tended to decrease CD4<sup>+</sup> and DN T cells (Fig. 5E). Populations of leukocytes present in the spleens of treated or sham-treated mice were compared <24 hours after administration of the last dose. Spleens from IMP-treated mice contained higher numbers of most leukocytes, especially PMNs, compared to PBS-treated mice (Supplementary Fig. S4), suggesting splenic sequestration may account for the decrease in corneal leukocyte populations in IMP-treated animals, as previously reported.<sup>26</sup>

While the absolute number of HVEM<sup>+</sup> cells in the cornea was lowered by IMP therapy (Fig. 5F), the proportion of HVEM<sup>+</sup> cells in the cornea was similar between treatments (Fig. 5G). Immune-modifying nanoparticle-treated mice had a significant decrease in the proportion of corneal HVEM<sup>+</sup> PMNs, compared to control, while the proportion of HVEM<sup>+</sup>

monocytes/macrophages and DCs increased (Fig. 5H). Proportions of lymphoid HVEM<sup>+</sup> populations did not vary significantly between the treatments (Fig. 5I). These data support the notion that HVEM<sup>+</sup> monocyte/macrophages and DCs in the cornea could derive from resident populations rather than from circulating pools, as IMP therapy did not affect, or even increase, their relative representation.

## DISCUSSION

In this study, we showed that HSV-1 infection acutely induces HVEM<sup>+</sup> expression on monocyte/macrophages in the cornea. Herpes virus entry mediator expression correlated with loss of corneal sensitivity and increased leukocytic infiltration, particularly in the chronic inflammatory phase of herpes stromal keratitis, which was ameliorated by ablation of HVEM from CD45<sup>+</sup> lineages. Finally, this work demonstrated that IMP therapy was useful in the treatment of murine HSK, as it prevented circulating leukocytes from invading the cornea and limited corneal sensation loss.

HVEM<sup>+</sup> populations in the cornea differed in the acute infectious stage from the chronic inflammatory phase, shifting from corneal monocyte-lineage cells to PMNs, DN T cells, and, as has been noted by others, CD4<sup>+</sup> T cells.<sup>35</sup> Because our current studies used only strain 17, we do not yet know whether these findings hold true for other HSV-1 strains; however, previous work from our laboratory using several different type 1 viruses, including the highly virulent McKrae,

indicates that HVEM-mediated pathogenesis is not strain-specific.<sup>21</sup> It would be informative to repeat our assessment of leukocytic infiltrates in WT corneas instead infected with HSV-1(McKrae), as this strain does not require scarification before infection to cause pathology.

In contrast to a prior report,<sup>22</sup> we were unable to detect significant levels of HVEM on corneal epithelial cells by IHC 1 dpi; flow cytometry 3 and 14 dpi indicated most (roughly 75%) HVEM<sup>+</sup> cells in the cornea were CD45<sup>+</sup> leukocytes. In a previous study using bone marrow chimeras with WT and HVEM KO mice, we have found that HVEM on radiation-resistant lineage(s) is sufficient to mediate disease after HSV infection.<sup>18</sup> The naïve cornea, once thought to be devoid of immune cells, contains numerous CD11b<sup>+</sup> cells with variable major histocompatibility complex (MHC) class II expression; most lack CD11c and Ly6G and therefore are of the monocyte/macrophage lineage.<sup>25,36</sup> Because a sizable portion (25%) of *in vivo* corneal resident macrophages do not turn over post irradiation even after 8 weeks of recovery,<sup>25</sup> we hypothesize that this cell type, essentially the only lineage to express HVEM early after infection, is the radiation-resistant population sufficient for HVEM-mediated HSV-1 pathogenesis.

Herpes virus entry mediator on corneal macrophages may promote immunopathogenesis by recruiting other inflammatory cells to the eye. Herpes virus entry mediator expression increases the levels of macrophage-associated chemotactic factors in the cornea, such as CXCL10 and CCL3, which are known to recruit PMNs, monocytes, and T cells during ocular HSV-1.<sup>18,37,38</sup> Herpes virus entry mediator upregulates these factors independently of viral entry,<sup>18</sup> consistent with the observation that, specifically in the cornea, levels of infectious virus do not correlate with chemokine expression.<sup>39</sup> In line with this hypothesis, we found that genetic ablation of HVEM from CD45<sup>+</sup> cells through a Cre/lox system prevented infiltration by myeloid cells and tended to limit CD4<sup>+</sup> populations. We also found that viral titers 1 dpi were higher in the control mice than in the conditional HVEM KOs, suggesting that HVEM on CD45<sup>+</sup> cells also has an early impact on viral replication. Herpes virus entry mediator increases viral titer independently of entry.<sup>18</sup> Herpes virus entry mediator on leukocytes may indirectly improve replication in or survival of infected corneal epithelial cells or fibroblasts, perhaps through increased expression of other HSV receptors or replication factors, although this mechanism requires further investigation.

In human patients with HSK, corneal sensitivity to mechanical stimulation is significantly impaired.<sup>40</sup> In our murine model, HVEM promoted loss of corneal sensitivity, which others have correlated with loss of sensory nerve endings from the cornea.<sup>41-43</sup> Immune cells and inflammatory mediators, such as IL-6, promote nerve retraction rather than direct effects of viral replication, and treatment with dexamethasone reduces corneal sensory nerve losses.<sup>41,42</sup> Some corneal monocytes/macrophages reside in close proximity to corneal nerve endings,<sup>44</sup> raising the intriguing possibility that resident HVEM<sup>+</sup> macrophages could aggravate nerve damage during acute infection. Consistent with this theory, WT mice had already begun losing corneal sensitivity, compared to HVEM KOs, as early as 2 to 3 dpi, at which time corneas contained significant HVEM<sup>+</sup> monocyte/macrophage cells but few other infiltrates, indirectly suggesting nerve damage precedes large-scale leukocyte invasion.

In fact, nerve damage likely contributes to further leukocytic infiltration of the cornea. Neuropeptides released from corneal nerve endings, such as substance P and calcitonin gene-related peptide, can induce IL-8 transcription in corneal epithelial cells, recruiting PMNs<sup>45,46</sup>; substance P has also been reported to increase the severity of HSK lesions.<sup>47</sup> Another

mechanism proposed by Yun and colleagues<sup>41</sup> posits that HSV (or, more likely, the initial inflammation associated with viral replication) damages corneal nerves, and subsequent desiccation due to lack of blinking leads to chronic, bilateral leukocytic infiltration. In addition, aberrantly organized sympathetic nerves have recently been found to invade the corneal stroma after sensory nerve retraction during HSV-1 infection.<sup>43</sup> The elimination of these fibers through superior cervical ganglionectomy reduces neovascularization and opacity, suggesting the influx of sympathetic fibers rather than a paucity of sensory fibers may be responsible for HSK symptoms.<sup>43</sup> In this study, we found that large populations of leukocytes in the cornea, especially PMNs and monocytes/macrophages, correlated with a prolonged lowered blink threshold 14 dpi. When HVEM ablation or treatment with IMPs 3 to 7 dpi prevented late-phase corneal infiltration, corneal sensitivity was preserved, suggesting nerve damage is exacerbated or perpetuated by PMN, CD4<sup>+</sup>, and other chronic-phase infiltrates.<sup>41</sup> Coincidentally, these populations were also HVEM<sup>+</sup>, although expression on these radiation-sensitive populations did not contribute significantly to pathogenesis in our earlier bone marrow chimera experiments.<sup>18</sup> We find it likely that both early and late inflammatory cells contribute to loss of corneal sensitivity during HSV infection: resident macrophages may secrete cytokines or other factors that damage corneal nerves, decreasing blinking and drying the eye, leading to immune cell infiltration, which in turn damages corneal nerves further.

Regardless of the precise recruitment mechanism of immune cells in the chronic phase, it is well established that their presence in the cornea promotes neoangiogenesis and neolymphangiogenesis,<sup>48,49</sup> opacification,<sup>50</sup> and scarring.<sup>51,52</sup> CD4<sup>+</sup> T cells also prevent reinnervation of the cornea, sustaining loss of the blink response and desiccation-related inflammation.<sup>41</sup> However, loss of immune cells, particularly macrophages, can be equally devastating, as unchecked viral replication leads to central nervous system (CNS) invasion and mortality: depletion of Gr-1<sup>+</sup> cells with a monoclonal antibody before and during infection increases replication, spread to the skin and brain, and mortality in BALB/c mice.<sup>53</sup> Clodronate liposomes, which nonspecifically deplete phagocytic cells including macrophages, injected subconjunctivally before infection severely heighten viral replication, blepharitis, and epithelial keratitis; however, stromal keratitis is mildly improved after depletion.<sup>54-56</sup> In contrast, delaying depletion to 2 and 4 dpi does not enhance viral replication.<sup>54</sup> These effects are likely due to macrophages, as targeted depletion of neutrophils with a Ly6G antibody does not alter viral replication or pathogenesis.<sup>57</sup>

Knowing this, we hypothesized that therapy in the prechronic phase (3-7 dpi) with IMPs, which are efficacious in the treatment of a host of inflammatory disorders,<sup>26,58</sup> could limit HSK symptoms without enhancing viral replication. Immune-modifying nanoparticles are absorbed by circulating engulfing cells; in inflammatory monocytes/macrophages, negatively charged particles are taken up in an opsonin-independent manner by the MARCO (macrophage receptor with collagenous structure) receptor.<sup>26</sup> This process redirects them to the spleen, where they undergo apoptosis, preventing tissue damage caused by these cells at extrasplenic sites.<sup>26</sup> In this study, the corneas of IMP-treated mice contained significantly fewer CD45<sup>+</sup> cells in general; both lymphoid (CD4<sup>+</sup>, natural killer T [NKT], and DN) and myeloid cell types (PMNs, monocytes, macrophages, and mDCs) were excluded from the cornea, with a concomitant preservation of corneal blink response. Initiation of treatment 3 dpi had no impact on viral loads, and actually improved mortality due to CNS involvement, indicating immune control of viral spread occurs within the first 72 hours after infection; after this, immune



populations in the cornea exacerbate rather than ameliorate pathology.<sup>4</sup>

Although previous work has focused on the role of IMPs in preventing inflammatory monocyte-driven pathology, in our model IMP therapy was also effective in limiting PMN, CD4<sup>+</sup> and DN T cells from the cornea.<sup>26</sup> There is some evidence that IMPs can act directly on these cell types,<sup>58</sup> although it is also possible that without inflammatory monocytes/macrophages in the cornea, T cell and neutrophil populations are not mobilized to the cornea. The characteristics and role of CD3<sup>+</sup>/CD4<sup>-</sup>/CD8<sup>-</sup> DN cells during HSK requires a more thorough investigation, as these cells could represent  $\gamma\delta$  T cells rather than true DN cells. Regardless, it is clear that IMP therapy limits their presence in the cornea. While acutely induced populations control viral spread, PMNs and macrophages in the chronic phase orchestrate much of HSK-related tissue damage.<sup>4,8,59</sup> Importantly, CD4<sup>+</sup> T cells are considered the primary pathologic cell type in HSK, and recent findings suggest depletion of this cell type allows for reversal of nerve loss and corneal damage.<sup>41</sup> Because IMP treatment significantly limited PMN and CD4<sup>+</sup> T cells in the cornea, this therapy would seem to be beneficial to the treatment of HSK inflammation.

In conclusion, we propose that HVEM on resident corneal monocytes/macrophages promotes early nerve damage, leading to increased infiltration of the cornea by a variety of leukocytes and furthering loss of corneal sensitivity. Interruption of this process, either by HVEM ablation from CD45<sup>+</sup> cells or by treatment with IMPs, prevents the influx of circulating immune cells, maintaining corneal health. Given these promising results, we are hopeful that IMP therapy could be adapted to treat recurrent HSK in human disease.

### Acknowledgments

The authors thank all the members of the Longnecker and Miller laboratories, especially Nanette Susmarski, for her assistance with cell culture, and Dan Xu, who prepared reagents for our use. They also thank Lin Li and the Northwestern University Mouse Histology and Phenotyping Laboratory, and the CCM Rodent (Preclinical) Technical Services Unit (RTSU) for their assistance with tail-vein injections. They also thank Sam Schaller and Rachel Riccio for their help counting plaques.

Supported by Training Program in Vision (T32 EY025202; RGE), National Institutes of Health (NIH) Grants R01EY023977-01A1 (SJK, RML), NIH R01NS026543 (SDM), NIH R01AI61516 (MK), National Multiple Sclerosis Society Postdoctoral Fellowship FG2065-A-1 (II), and Crohn's and Colitis Foundation of America Fellowship (J-WS). The funders had no role in the design of the studies, the collection or interpretation of the data, or the decision to submit the work for publication.

Disclosure: **R.G. Edwards**, None; **S.J. Kopp**, None; **I. Ifergan**, None; **J.-W. Shui**, None; **M. Kronenberg**, None; **S.D. Miller**, None; **R. Longnecker**, None

### References

- Chayavichitsilp P, Buckwalter JV, Krakowski AC, Friedlander SF. Herpes simplex. *Pediatr Rev.* 2009;30:119-129.
- Biswas PS, Rouse BT. Early events in HSV keratitis—setting the stage for a blinding disease. *Microbes Infect.* 2005;7:799-810.
- Deshpande S, Banerjee K, Biswas PS, Rouse BT. Herpetic eye disease: immunopathogenesis and therapeutic measures. *Expert Rev Mol Med.* 2004;6:1-14.
- Streilein J, Reza Dana M, Ksander B. Immunity causing blindness: five different paths to herpes stromal keratitis. *Immunology Today.* 1997;18:443-449.
- Su YH, Yan XT, Oakes JE, Lausch RN. Protective antibody therapy is associated with reduced chemokine transcripts in herpes simplex virus type 1 corneal infection. *J Virol.* 1996;70:1277-1281.
- Thomas J, Kanangat S, Rouse BT. Herpes simplex virus replication-induced expression of chemokines and proinflammatory cytokines in the eye: implications in herpetic stromal keratitis. *J Interferon Cytokine Res.* 1998;18:681-690.
- Babu JS, Thomas J, Kanangat S, Morrison LA, Knipe DM, Rouse BT. Viral replication is required for induction of ocular immunopathology by herpes simplex virus. *J Virol.* 1996;70:101-107.
- Thomas J, Gangappa S, Kanangat S, Rouse BT. On the essential involvement of neutrophils in the immunopathologic disease herpetic stromal keratitis. *J Immunol.* 1997;158:1383-1391.
- Gangappa S, Deshpande S, Rouse BT. Bystander activation of CD4<sup>+</sup> T cells accounts for herpetic ocular lesions. *Invest Ophthalmol Vis Sci.* 2000;41:453-459.
- Montgomery RI, Warner MS, Lum BJ, Spear PG. Herpes simplex virus-1 entry into cells mediated by a novel member of the TNF/NGF receptor family. *Cell.* 1996;87:427-436.
- Yoon M, Zago A, Shukla D, Spear PG. Mutations in the N termini of herpes simplex virus type 1 and 2 gDs alter functional interactions with the entry/fusion receptors HVEM, nectin-2, and 3-O-sulfated heparan sulfate but not with nectin-1. *J Virol.* 2003;77:9221-9231.
- Yoon M, Spear PG. Random mutagenesis of the gene encoding a viral ligand for multiple cell entry receptors to obtain viral mutants altered for receptor usage. *Proc Natl Acad Sci U S A.* 2004;101:17252-17257.
- Akhtar J, Tiwari V, Oh MJ, et al. HVEM and nectin-1 are the major mediators of herpes simplex virus 1 (HSV-1) entry into human conjunctival epithelium. *Invest Ophthalmol Vis Sci.* 2008;49:4026-4035.
- Shukla SY, Singh YK, Shukla D. Role of nectin-1, HVEM, and PILR-alpha in HSV-2 entry into human retinal pigment epithelial cells. *Invest Ophthalmol Vis Sci.* 2009;50:2878-2887.
- Satoh T, Arase H. HSV-1 infection through inhibitory receptor, PILRalpha. *Virus.* 2008;58:27-36.
- Bosnjak L, Miranda-Saksena M, Koelle DM, Boadle RA, Jones CA, Cunningham AL. Herpes simplex virus infection of human dendritic cells induces apoptosis and allows cross-presentation via uninfected dendritic cells. *J Immunol.* 2005;174:2220-2227.
- Karaba AH, Kopp SJ, Longnecker R. Herpesvirus entry mediator and nectin-1 mediate herpes simplex virus 1 infection of the murine cornea. *J Virol.* 2011;85:10041-10047.
- Edwards RG, Kopp SJ, Karaba AH, Wilcox DR, Longnecker R. Herpesvirus entry mediator on radiation-resistant cell lineages promotes ocular herpes simplex virus 1 pathogenesis in an entry-independent manner. *MBio.* 2015;6:e01532-15.
- Yoon M, Kopp SJ, Taylor JM, Storti CS, Spear PG, Muller WJ. Functional interaction between herpes simplex virus type 2 gD and HVEM transiently dampens local chemokine production after murine mucosal infection. *PLoS One.* 2011;6:e16122.
- Kopp SJ, Storti CS, Muller WJ. Herpes simplex virus-2 glycoprotein interaction with HVEM influences virus-specific recall cellular responses at the mucosa. *Clin Dev Immunol.* 2012;2012:284104.
- Karaba AH, Kopp SJ, Longnecker R. Herpesvirus entry mediator is a serotype specific determinant of pathogenesis in ocular herpes. *Proc Natl Acad Sci U S A.* 2012;109:20649-20654.
- Kovacs SK, Tiwari V, Prandovszky E, et al. Expression of herpes virus entry mediator (HVEM) in the cornea and

- trigeminal ganglia of normal and HSV-1 infected mice. *Curr Eye Res.* 2009;34:896-904.
23. Murphy KM, Nelson CA, Sedy JR. Balancing co-stimulation and inhibition with BTLA and HVEM. *Nat Rev Immunol.* 2006;6:671-681.
  24. Heo SK, Ju SA, Lee SC, et al. LIGHT enhances the bactericidal activity of human monocytes and neutrophils via HVEM. *J Leukoc Biol.* 2006;79:330-338.
  25. Chinnery HR, Humphries T, Clare A, et al. Turnover of bone marrow-derived cells in the irradiated mouse cornea. *Immunology.* 2008;125:541-548.
  26. Getts DR, Terry RL, Teague Getts, et al. Therapeutic inflammatory monocyte modulation using immune-modifying microparticles. *Sci Trans Med.* 2014;6:1-14.
  27. Chucair-Elliott AJ, Zheng M, Carr DJ. Degeneration and regeneration of corneal nerves in response to HSV-1 infection. *Invest Ophthalmol Vis Sci.* 2015;56:1097-1107.
  28. Chen W, Tang Q, Hendricks RL. Ex vivo model of leukocyte migration into herpes simplex virus-infected mouse corneas. *J Leukoc Biol.* 1996;60:167-173.
  29. Osorio Y, Wechsler SL, Nesburn AB, Ghiasi H. Reduced severity of HSV-1 induced corneal scarring in IL-12-deficient mice. *Virus Res.* 2002;90:317-326.
  30. Rowe AM, St Leger AJ, Jeon S, Dhaliwal DK, Knickelbein JE, Hendricks RL. Herpes keratitis. *Prog Retin Eye Res.* 2013;32:88-101.
  31. Abram CL, Roberge GL, Hu Y, Lowell CA. Comparative analysis of the efficiency and specificity of myeloid-Cre deleting strains using ROSA-EYFP reporter mice. *J Immunol Methods.* 2014;408:89-100.
  32. Egan KP, Wu S, Wigdahl B, Jennings SR. Immunological control of herpes simplex virus infections. *J Neurovirol.* 2013;19:328-345.
  33. Frank GM, Buella KA, Maker DM, Harvey SA, Hendricks RL. Early responding dendritic cells direct the local NK response to control herpes simplex virus 1 infection within the cornea. *J Immunol.* 2012;188:1350-1359.
  34. Daheshia M, Kanangat S, Rouse BT. Production of key molecules by ocular neutrophils early after herpetic infection of the cornea. *Exp Eye Res.* 1998;67:619-624.
  35. Sharma S, Rajasagi NK, Veiga-Parga T, Rouse BT. Herpes virus entry mediator (HVEM) modulates proliferation and activation of regulatory T cells following HSV-1 infection. *Microbes Infect.* 2014;16:648-660.
  36. Brissette-Storkus CS, Reynolds SM, Lepisto AJ, Hendricks RL. Identification of a novel macrophage population from normal mouse corneal stroma. *Invest Ophthalmol Vis Sci.* 2002;43:2264-2271.
  37. Carr DJJ, Chodosh J, Ash J, Lane TE. Effect of anti-CXCL10 monoclonal antibody on herpes simplex virus type 1 keratitis and retinal infection. *J Virol.* 2003;77:10037-10046.
  38. Carr DJ, Tomanek L. Herpes simplex virus and the chemokines that mediate the inflammation. *Curr Top Microbiol Immunol.* 2006;303:47-65.
  39. Carr DJ, Campbell IL. Herpes simplex virus type 1 induction of chemokine production is unrelated to virus load in the cornea but not in the nervous system. *Viral Immunol.* 2006;19:741-746.
  40. Gallar J, Tervo TM, Neira W, et al. Selective changes in human corneal sensation associated with herpes simplex virus keratitis. *Invest Ophthalmol Vis Sci.* 2010;51:4516-4522.
  41. Yun H, Rowe AM, Lathrop KL, Harvey SA, Hendricks RL. Reversible nerve damage and corneal pathology in murine herpes simplex stromal keratitis. *J Virol.* 2014;88:7870-7880.
  42. Chucair-Elliott AJ, Jinkins J, Carr MM, Carr DJ. IL-6 contributes to corneal nerve degeneration after herpes simplex virus type 1 infection. *Am J Pathol.* 2016;186:2665-2678.
  43. Yun H, Lathrop KL, Hendricks RL. A central role for sympathetic nerves in herpes stromal keratitis in mice. *Invest Ophthalmol Vis Sci.* 2016;57:1749-1756.
  44. Seyed-Razavi Y, Chinnery HR, McMenamin PG. A novel association between resident tissue macrophages and nerves in the peripheral stroma of the murine cornea. *Invest Ophthalmol Vis Sci.* 2014;55:1313-1320.
  45. Tran MT, Lausch RN, Oakes JE. Substance P differentially stimulates IL-8 synthesis in human corneal epithelial cells. *Invest Ophthalmol Vis Sci.* 2000;41:3871-3877.
  46. Tran MT, Ritchie MH, Lausch RN, Oakes JE. Calcitonin gene-related peptide induces IL-8 synthesis in human corneal epithelial cells. *J Immunol.* 2000;164:4307-4312.
  47. Twardy BS, Channappanavar R, Suvas S. Substance P in the corneal stroma regulates the severity of herpetic stromal keratitis lesions. *Invest Ophthalmol Vis Sci.* 2011;52:8604-8613.
  48. Conrady CD, Zheng M, Stone DU, Carr DJ. CD8+ T cells suppress viral replication in the cornea but contribute to VEGF-C-induced lymphatic vessel genesis. *J Immunol.* 2012;189:425-432.
  49. Gimenez F, Suryawanshi A, Rouse BT. Pathogenesis of herpes stromal keratitis—a focus on corneal neovascularization. *Prog Retin Eye Res.* 2013;33:1-9.
  50. Divito SJ, Hendricks RL. Activated inflammatory infiltrate in HSV-1-infected corneas without herpes stromal keratitis. *Invest Ophthalmol Vis Sci.* 2008;49:1488-1495.
  51. Allen SJ, Mott KR, Ljubimov AV, Ghiasi H. Exacerbation of corneal scarring in HSV-1 gK-immunized mice correlates with elevation of CD8+CD25+ T cells in corneas of ocularly infected mice. *Virology.* 2010;399:11-22.
  52. Allen SJ, Mott KR, Ghiasi H. Overexpression of herpes simplex virus glycoprotein K (gK) alters expression of HSV receptors in ocularly-infected mice. *Invest Ophthalmol Vis Sci.* 2014;55:2442-2451.
  53. Tumpey TM, Chen S-H, Oakes JE, Lausch RN. Neutrophil-mediated suppression of virus replication after herpes simplex virus type 1 infection of the murine cornea. *J Virol.* 1996;70:898-904.
  54. Cheng H, Tumpey TM, Staats HF, van Rooijen N, Oakes JE, Lausch RN. Role of macrophages in restricting herpes simplex virus type 1 growth after ocular infection. *Invest Ophthalmol Vis Sci.* 2000;41:1402-1409.
  55. Mott K, Brick DJ, van Rooijen N, Ghiasi H. Macrophages are important determinants of acute ocular HSV-1 infection in immunized mice. *Invest Ophthalmol Vis Sci.* 2007;48:5605-5615.
  56. Conrady CD, Zheng M, Mandal NA, van Rooijen N, Carr DJ. IFN-alpha-driven CCL2 production recruits inflammatory monocytes to infection site in mice. *Mucosal Immunol.* 2013;6:45-55.
  57. Wojtasiak M, Pickett DL, Tate MD, et al. Depletion of Gr-1+, but not Ly6G+, immune cells exacerbates virus replication and disease in an intranasal model of herpes simplex virus type 1 infection. *J Gen Virol.* 2010;91:2158-2166.
  58. Getts DR, Shea LD, Miller SD, King NJ. Harnessing nanoparticles for immune modulation. *Trends Immunol.* 2015;36:419-427.
  59. Bauer D, Mryzk S, van Rooijen N, Steuhl K, Heiligenhaus A. Macrophage-depletion influences the course of murine HSV-1 keratitis. *Curr Eye Res.* 2000;20:45-53.